Transient plasma potential in pulsed dual frequency inductively coupled plasmas and effect of substrate biasing

Anurag Mishra and Geun Young Yeom'

Citation: AIP Advances **6**, 095101 (2016); doi: 10.1063/1.4961940
View online: http://dx.doi.org/10.1063/1.4961940
View Table of Contents: http://aip.scitation.org/toc/adv/6/9
Published by the American Institute of Physics

Transient plasma potential in pulsed dual frequency inductively coupled plasmas and effect of substrate biasing

Anurag Mishra[1] and Geun Young Yeom[1,2,a]
[1]*Department of Advanced Materials Science and Engineering, Sungkyunkwan University, Suwon, Gyeonggi-do, 440-746, South Korea*
[2]*SKKU Advanced Institute of Nanotechnology(SAINT), Sungkyunkwan University, Suwon, Gyeonggi-do, 440-746, South Korea*

(Received 17 March 2016; accepted 15 August 2016; published online 2 September 2016)

An electron emitting probe in saturated floating potential mode has been used to investigate the temporal evolution of plasma potential and the effect of substrate RF biasing on it for pulsed dual frequency (2 MHz/13.56 MHz) inductively coupled plasma (ICP) source. The low frequency power (P_{2MHz}) has been pulsed at 1 KHz and a duty ratio of 50%, while high frequency power ($P_{13.56MHz}$) has been used in continuous mode. The substrate has been biased with a separate bias power at ($P_{12.56MHz}$) Argon has been used as a discharge gas. During the ICP power pulsing, three distinct regions in a typical plasma potential profile, have been identified as 'initial overshoot', pulse 'on-phase' and pulse 'off-phase'. It has been found out that the RF biasing of the substrate significantly modulates the temporal evolution of the plasma potential. During the initial overshoot, plasma potential decreases with increasing RF biasing of the substrate, however it increases with increasing substrate biasing for pulse 'on-phase' and 'off-phase'. An interesting structure in plasma potential profile has also been observed when the substrate bias is applied and its evolution depends upon the magnitude of bias power. The reason of the evolution of this structure may be the ambipolar diffusion of electron and its dependence on bias power.
[http://dx.doi.org/10.1063/1.4961940]

I. INTRODUCTION

Plasma processing plays a major role in various applications such semiconductor manufacturing, display panels solar cells etc.[1–3] As the number of transistors in a single chip is increasing by a factor of ~ 2 in a year and therefore device size is continuously shrinking, that results in increasing fabrication cost. To optimize the fabrication cost, it is necessary to do plasma processing at large area wafer. However, scaling-up the wafer size poses few technological challenges. When radial dimension of wafer becomes comparable to wavelength of applied frequency, the standing waves generates in the discharge, which results in discharge non-uniformity in radial direction. Secondly, it is of utmost important to have a separate control over ion flux and ion energy to have damage free tailored discharge processes.[4,5]

Single frequency capacitive discharges do not allow ion flux and ion energies to be varied separately. Goto *et al*. proposed that the dual frequency capacitively coupled plasma (CCP) excitation operating at substantially different frequencies, e.g. 2 and 27 MHz might offer this kind of control.[6] However, it has been found out later that the quality of the separate control of ion energy and flux in dual frequency CCP discharges is limited due to the coupling of both frequencies[7–9] and the capacitive sheath effect, which increases both ion energy and plasma density together.[10,11] In order

[a]Author for correspondence Email: gyyeom@skku.edu

to obtain better control of ion energy and ion flux at the substrate, triple frequency CCP discharges operated at substantially different frequencies[12,13] have also been investigated. However, using high frequency (in order to have decoupling between ion flux and ion energy) introduces electromagnetic (standing wave) effects and therefore poses another issue of discharge non-uniformity over the substrate, when wavelength of applied frequency becomes comparable to the substrate radial dimension.[14–17]

Inductive discharges may be useful to overcome these limitations, in which the plasma is produced by an RF current in an external coil while the wafer-holder is biased by an independent power supply. Recently, a new type of ICP source based on utilizing dual-antenna, dual frequency concept has been proposed and a discharge non-uniformity of ~4% has been achieved over the substrate area, 450 mm in diameter.[18] By using this kind of plasma source, it has also been demonstrated that ion and electron energy distribution could be efficiently modulated by varying two power ratio.[19,20]

A further advantage, such as more flexibility to control the discharge parameters, could be added, if this source is used in a pulsed mode.[18] Pulsed plasmas show significant potential to meet the majority of the scaling challenges and offer new tuning knobs (pulse frequency, duty cycle, and optional phase lag between source and bias pulses) that enhance independent control of plasma conditions (in particular, ion bombardment energy and plasma chemical composition. Several pulsing modes can be envisaged. For example, either only the source or the bias generator is pulsed, both bias and source are simultaneously pulsed (synchronous pulsing) with or without time delay between them. Since power is actively deposited for only a fraction of the time, pulsed plasmas offer the possibility of working with low ion energy regimes (below 5 eV), less charging, and with less dissociated (and less reactive) plasmas, resulting in a better process performance in terms of damage, selectivity, and profile control. The control over ion bombarding energies could further be controlled by applying RF bias at the substrate.

Plasma potential is important discharge parameters that not only provides information about the electric field structure within the plasma but also determines, together with sheath potential across the sheath, ion bombarding energies over the floated or grounded substrate.

Emissive probe technique has been proved to be very useful for investigating of temporal evolution of plasma potential for pulsed plasmas. This technique can be used in three different ways, that is, separation point mode, inflection point mode, and the floating point (saturated floating potential) mode.[21] Among these modes, due to inherent simplicity in using and real time measurements of time resolved plasma potential, the floating point technique has been extensively used, particularly in pulsed plasmas.[25–29] The working principal of emissive probe in this mode of operation is as follows. As the probe surface becomes strongly electron emitting, floating potential of probe moves to meet the plasma potential. According to a theory that ignores the existence of pre-sheath, the floating potential measured by emissive probe in strongly emitting condition saturates T_e/e below the plasma potential at the sheath edge, when space charge effects are taken into account.[23] Here, T_e and 'e' are electron temperature and electronic charge respectively. A computation study, based on particle-in-cell (PIC) simulations, predicts this offset between plasma potential and floating potential of probe depends on electron temperature and may be upto 1.5 T_e/e. The studies performed demonstrate that the floating potential of an emitting probe is always lower than plasma potential by an amount of ~1.5 T_e. The magnitude of associated error can be determined by relative magnitude of plasma potential to electron temperature (eV_p/T_e).[21] If the electron temperature is high enough and close to plasma potential, this offset in plasma potential can be significant. In the present experimental study, typical plasma potential, during pulse 'on-time', is ~40 V and the electron temperature measured by Langmuir probe (not shown here) is ~4 eV, thererefore the offset in plasma potential due to error associated with emissive probe technique in floating point method is not significant. Few more studies revealed that applicability of floating potential mode of emissive probe in low temperature plasma depends upon the ratio of T_e/T_{ew} and on plasma density (n_e), where T_e and T_{ew} are plasma electron temperature and temperature of emitting electron from probe loop.[30,31] A 1-D model has been applied to understand the potential difference between strongly emitting wall (probe loop) and plasma potential and it has been demonstrated that if T_e and T_{ew} are comparable, the plasma potential determined by strongly emitting probe can be significantly over-estimated and if T_e is significantly higher than T_{ew}.[31] The plasma potential measured in present

study is few tens of volts and assuming temperature of emitting electron ~ 0.3 eV,[31] it can be fairly said that plasma potential measurements are under-estimated by an amount of $kT_e/_e$. Another source of error comes from using the emissive probe in RF plasmas. Wang *et al*.[24] showed that, depending upon the load resistor, the impedance across which the probe current is measured, the floating potential may follow the average plasma potential, however it could also vary with RF voltage. Nevertheless, this technique is very useful in measuring the plasma potential in pulsed plasmas and provides accurate and quick qualitative information about the temporal evolution of plasma potential. The usefulness of the technique to accurately determine V_p throughout the pulsed plasma, has already been demonstrated.[25–27] The details of working principle and design of the emissive probe can be found elsewhere.[21,23,25–27]

The present study investigates the temporal evolution of plasma potential and the effect of substrate biasing on it, in the pulsed discharges produced by a dual-frequency/dual-antenna ICP source by using an emissive probe. The plasma potential has been measured using a Tektronix voltage probe TPP0201 (input impedance of 10 MΩ, oscilloscope impedance).

II. EXPERIMENTAL ARRANGEMENT

A schematic of the experimental system has been shown in figure 1. A cylindrical stainless steel chamber, with the inner diameter of 650 mm and the height of 400 mm, has been used in this study. A 35 mm thick quartz window is used to cover the top side of the processing chamber and to hold the ICP source. The ICP source consists of two spiral coils. The inner coil (thirteen turns having diameter of 400 mm) and outer coil (two turns) are energized by 2 (P_{2MHz}) and 13.56MHz ($P_{13.56MHz}$) RF powers, respectively. The P_{2MHz} has been applied by a signal generator (HP 8657B) and 1 kW RF power amplifier (ENI A1000, 0.3 – 35 MHz) and pulsed by a pulse generator (HP 8116A), whereas $P_{13.56MHz}$ has been applied by an RF power generator (CX-5000S, COMDEL) via automatic matching network. Both RF powers (P_{2MHz} and $P_{13.56MHz}$) have been varied from 200 W to 600 W with a step of 200 W. The substrate has been biased by a separate RF generator (RF20R supplied by Advanced Energy) and the biasing power has been varied from 0 to 250 W with a step of 50 W. Argon gas has been uniformly distributed inside the chamber via a multi-hole shower head located at the circumference of the vacuum chamber. The separation between the plasma source and the substrate is 90 mm. The chamber walls are electrically grounded. The pressure inside the chamber has been controlled by using a mass flow controller (2900 series, Tylan) together with an

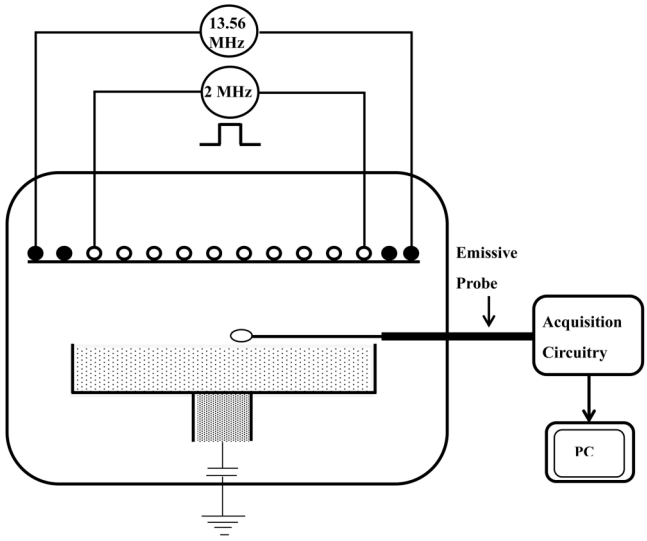

FIG. 1. A schematic of the experimental set-up of pulsed dual frequency ICP system used in present study. The inner coil has been energized by a pulsed 2 MHz rf power and the outer coil by a continuous wave 13.56 MHz rf power.

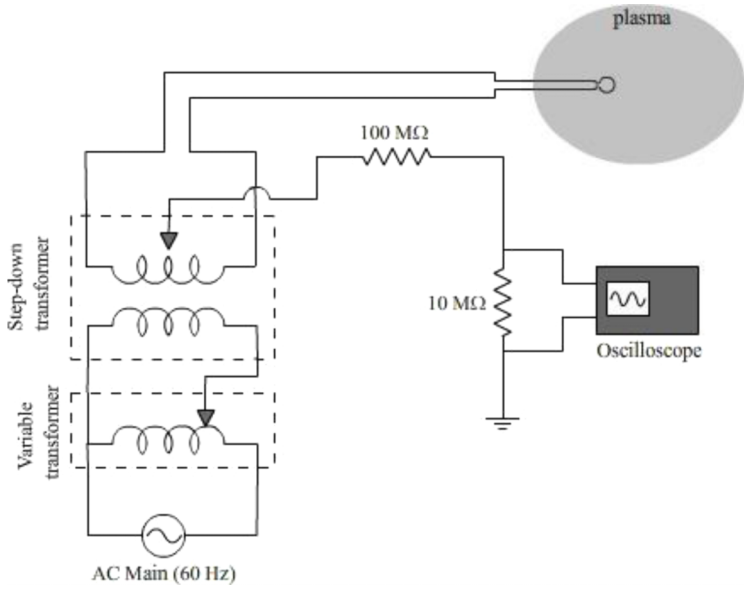

FIG. 2. A schematic of emissive probe electrical arrangement.

adaptive pressure controller (PM-7, VAT) for the gate valve control. The operating pressure is kept constant at 10 mTorr for most of the measurements.

The emissive probe electrical arrangement is shown in figure 2. The probe is located at the center of discharge, 70 mm away from the plasma source and 20 mm above the substrate. The emissive probe was made of a thoriated tungsten wire of diameter 125 μm, looped in a semicircle of 2 mm diameter and push-fitted into a ceramic stem housing with enameled copper connecting wires of 250 μm diameter that carry the external heating current. The probe loop was heated by passing through it a 60 Hz ac current supplied by a two-stage transformer circuit. The center tap of the second transformer was connected to a fast oscilloscope (DSO7054A, 1MΩ input impedance, InfiiVision, Agilent Ltd.) via a 10× voltage probe (TPP0201, Tektronix Ltd.) to obtain the mean voltage (floating potential) across the loop and hence a good estimate of V_p. This floating potential data were stored over 512 discharges pulses and then averaged to minimize the random error in the electrical signal. The heating current has been measured by current transformer monitor, model 6650 by Pearson Electronics, USA.

In order to ensure that the probe is always in a strongly emitting condition, a change in floating potential of the probe with respect to probe current (heating current) has been measured. For pulsed ICP plasmas, three phases have been identified in the temporal evolution of floating potential profile as 'initial overshoot', stable 'on-phase', and stable 'off-phase' as shown in figure 3. The potentials variation, for the three identified phases, as a function of the probe current are shown in figure 4. The data has been sampled at a typical discharge condition (P_{2MHz} = $P_{13.56MHz}$ = 200 W, $P_{12.56MHz}$ = 100 W, Ar pressure = 10 mTorr). When the probe was cold (no heating current), the floating potential during all three phases, is ~10 V. Electron emission from the probe increases with heating current and that, in turn, increases the floating potential to meet the plasma potential. The floating potential saturates at ~ 60, ~39 and ~44 V in three phases- 'initial overshoot', stable 'on-phase' and stable 'off-phase', respectively, at the probe current of ~0.9 A. A relatively high probe current (~1.2 A) has been used in all the experiments to ensure that the probe is always in strongly emitting condition so that the probe potential should be approximately equal to the plasma potential.

To benchmark emissive probe measurements, the V_f profile has also been measured by a non-compensated Langmuir probe at same conditions and location in plasma and compared with the floating potential measured by emissive probe. It has been found that the floating potential measured by emissive probe is in good agreement with Langmuir probe measurements as explained elsewhere.[22]

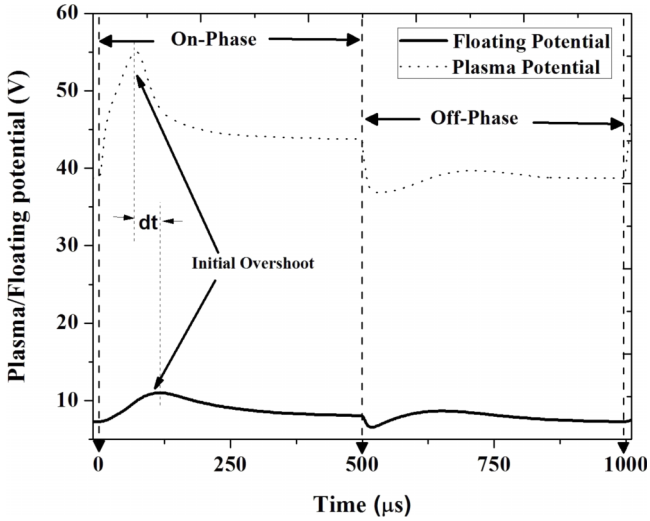

FIG. 3. A plot of temporal evolution of plasma potential and floating potential. In the plot, three phases (Initial Overshoot, 'On-phase' and 'Off-phase') have been shown. These potential profiles have been acquired at P_{2MHz} = $P_{13.56MHz}$ = 200 W, $P_{12.56MHz}$ = 100 W, Ar P = 10 mTorr.

III. RESULTS AND DISCUSSION

A. Temporal evolution of plasma potential

A plot of temporal evolution of plasma and floating potential measured at a particular condition (P_{2MHz} = $P_{13.56MHz}$ = 200 W, P_{2MHz} pulse frequency/duty percentage= 1 kHz/50%), substrate bias power $P_{12.56MHz}$ = 100 W, Ar pressure = 10 mTorr,) has been shown in figure 3 and three phases, (1) initial overshoot, (2) stable 'on-phase' and (3) almost stable 'off-phase' have also been indicated in the plot. For the analysis, time t=0 μs has been defined as the time when P_{2MHz} pulse switches on. The plasma potential achieves an 'initial overshoot' of ~68 V at a time of ~72 μs after the

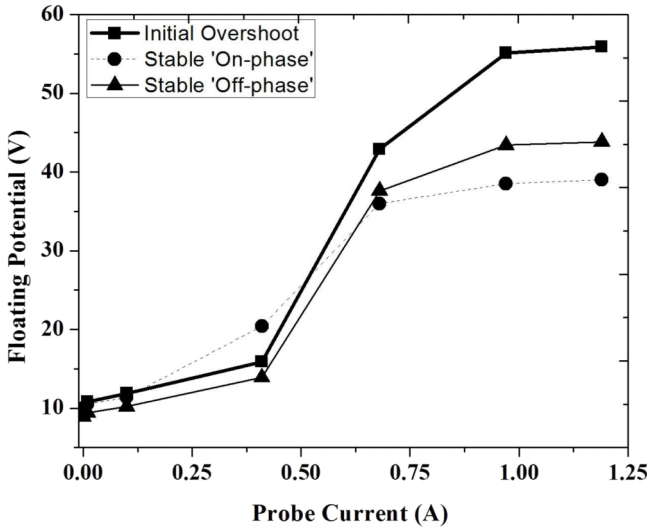

FIG. 4. A plot of measured emissive probe floating potential (V_f) versus loop heat current (I_h) at one position (r= 00 mm, z= -20 mm) during three identified phases in the V_f waveform: (a) the 'initial overshoot' (b) pulse 'on-time' and (c) pulse 'off-time' as described in Figure 3. It should be noted that, at I_L ~ 1.0 A, the floating potential V_f approaches to the plasma potential V_p. All the measurements have been carried at P_{2MHz}=$P_{13.56MHz}$ = 200 W, $P_{12.56MHz}$ = 100 W and Ar pressure of 10 mTorr.

initiation of P_{2MHz} pulse, then stabilizes at t~170 μs and remains stable at ~45 V for remaining pulse 'on-time'. The plasma potential gets a depression of ~ 10 V as the pulse switches off and then remains stable at ~36 V within ± 2 volts for the rest of the pulse 'off-time as to the $P_{13.56MHz}$ and $P_{12.56MHz}$ were still on during the pulse off-time. The reason of 'initial overshoot' can be attributed to discharge dynamics and capacitive effect associated with sheath around the probe loop that determines the time response of the probe. From the electrical equivalent circuit of the plasma probe measurement, in which a parallel combination of sheath resistance (R_{sh}) and sheath capacitance ($C_{sh,} = \varepsilon_0 A/d$, where A is the probe area and d is the sheath width) are connected to ground via a cable capacitance (C_g), the probe response time (τ) can be given by $\tau = R_{sh}Z_{sh}C_g/(R_{sh}+Z_{sh})$,[32] where $Z_{sh}=1/\omega Cs_h$. Bradley *et al*. reported that the probe response time τ can be simply expressed by the time constant of charging the capacitance of probe set-up to ground C_g via sheath resistance R_{sh} i.e. $\tau = R_{sh}C_g$.[28] As proposed by Welzel *et al*.,[33] sheath resistance can be calculated by the ratio of voltage drop between probe and bulk plasma (k_BT_e) and the electron thermal current through the sheath ($A_p e n_e \sqrt{\frac{k_BT_e}{2\pi m_e}}$), when electron density (n_e) and the electron temperature (T_e) are known. By taking precautions, the probe setup capacitance to ground could be reduced upto ~220 pF. Assuming the electron density in order of 10^{17} m^{-3} and the electron temperature of 3-5 eV, the probe response time comes out to ~ 150 ns. However, during the initiation of discharge pulse, the electron density and electron temperature are much lower typically $n_e \sim 10^{14}$ -10^{15} m^{-3} and 5 eV, respectively, and the temporal resolution of probe becomes ~ 20-100 μs. Hence, this emissive probe set-up is not capable to provide the correct information about true plasma potential during discharge transition i.e. off-on and on-off transitions. Therefore, the overshooting/undershooting structure in plasma potential during these transition period mostly depends upon the capacitive effects originated due to the probe set-up. When the probe is in no emission condition, the sheath (measuring floating potential) around the probe is thick, and therefore sheath resistance R_{sh} increases that, in turn, reduces the temporal resolution of the probe. That is the reason that a time lag between initial overshoot in plasma and floating potential is observed (fig. 3). The comparison of plasma potential and floating potential profiles (fig. 3) readily reveals the initial peak in the floating potential profile occurs after the occurrence of 'initial overshoot' in the plasma potential with a time lag (dt) of ~40 μs. This observed time lag is the result of probe response time to the fluctuations occurring in the discharge (τ), which depends on the sheath resistance and capacitance of probe setup to ground as mentioned earlier. The time of occurrence of 'initial overshoot' in floating potential with the probe current is shown in figure 5 for the discharge condition shown in figure 3. As shown, it is evident that the time of occurrence initial overshoot decreases (probe resolution increases) with the

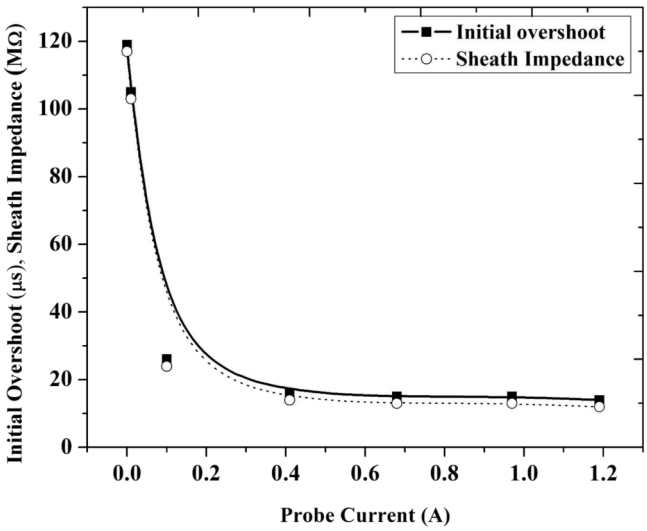

FIG. 5. A plot of time of occurrence of 'Initial Overshoot' and sheath impedance with probe loop heating current. The discharge condition is $P_{2MHz} = P_{13.56MHz} = 200$ W, $P_{12.56MHz} = 100$ W, Ar P = 10 mTorr.

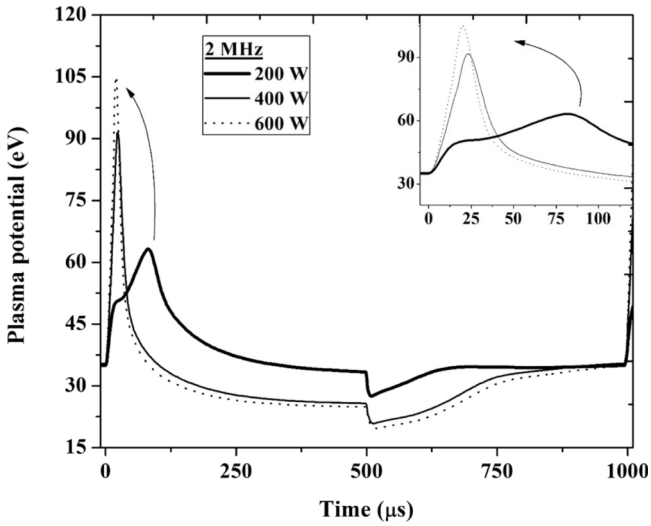

FIG. 6. A plot of temporal evolution of plasma potential with P_{2MHz}. All the measurements have been carried, $P_{13.56MHz}$ = 200 W, at $P_{12.56MHz}$= 00 W and Ar pressure of 10 mTorr.

probe loop current. Important information about the evolution of sheath impedance with the probe current can also be extracted from figure 5. From the previous equation related to the probe response time, the effective sheath impedance, can be approximates as τ/C_{cg}. Therefore, a plot of τ/C_{cg} versus probe current yields the evolution of sheath impedance with probe current and redrawn in figure 5. It gives, as mentioned above, Z_p is independent of probe current, therefore, $R_{sh}C_{sh} \alpha \tau$.

The temporal evolution of plasma potential with pulsed P_{2MHz} ($P_{13.56MHz}$ =200 W) with no substrate biasing ($P_{12.56MHz}$ = 00 W) is shown in Figure 6. To investigate initial transients in plasma potential profile more precisely, a zoomed in part of initial evolution is also shown in inset. The time of occurrence of 'initial peak' in plasma potential decreases with P_{2MHz}, from 80 μs to 19 μs as P_{2MHz} increases from 200 to 600 W and is attributed to increasing temporal resolution of the probe response due to increasing plasma density, which reduces the sheath resistance. The magnitude of 'initial peak' increases with increasing P_{2MHz}. In the beginning of pulse, the plasma density is very low ($\sim 10^{14}$ m^{-3}) and the discharge is in a capacitive mode. Therefore, RF voltage on the antenna coils increases with increasing P_{2MHz} that in turn increases the plasma potential. However, the plasma potential decreases with P_{2MHz} during the rest of the 'on-phase' and it is common to glow discharges and due to increasing ionization at higher plasma density (higher RF power). As soon as P_{2MHz} switches off, the plasma potential gets a depression of few volts (~5 V) and then increases slowly up-to 150 to 300 μs (depending on P_{2MHz}) and then stabilizes. This increasing trend in the plasma potential just after P_{2MHz} switches can be explained on the basis of charged particles diffusion. Plasma potential can be determined from the Poisson relation and depends upon electron and ion density i.e. proportional to $\sim(n_e - n_i)$. Due to higher mobility of electrons, electrons tend to diffuse faster than ions and this imbalance between electron and ion density ($n_e - n_i$) at a particular position is responsible for the value of plasma potential. Assuming that electrons and ions are un-magnetized, electrons are more mobile than ions and no particle generation during the pulse off time, The ambipolar diffusion coefficient can be given by $D_a = D_i (1 + T_e/T_i) \sim kT_e/M\upsilon$, where, D_i is ion diffusion coefficient, T_e electron temperature, Ti ion temperature, M ion mass and υ ion neutral collision frequency for the momentum transfer.[5] Considering a symmetric dimension of 2L (where L is radius of chamber), a time dependent solution of diffusion equation yields the decay time constant $\tau_0 = (2L/\pi)^2.(1/D_a)$. Assigning a precise value for υ is difficult as it requires a good description of ion dynamics. Typically, at pressure of 10 mTorr and electron temperature of 3 eV, the estimated D_a is 2 x 10^3 m^2 s^{-1} and it yield $\tau_0 \sim 50$ μs. In our experimental study, there is a source ($P_{13.56MHz}$) during the pulse off duration and it increases diffusion time constant. Also, as P_{2MHz} increases during the pulse on-time, the remaining plasma density during the pulse off-time

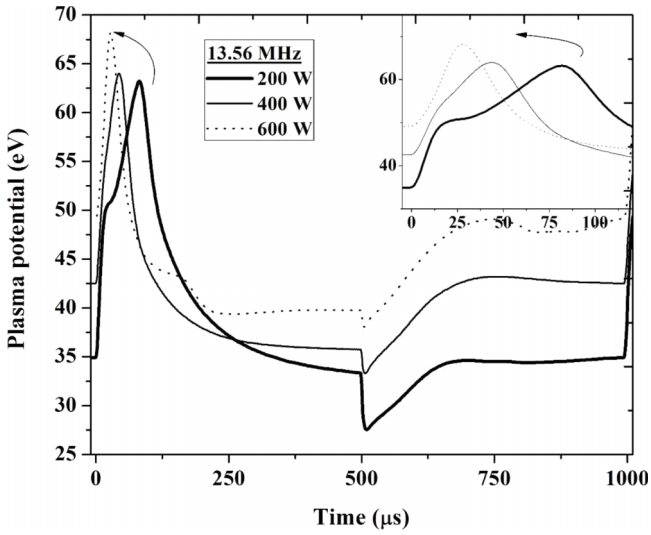

FIG. 7. A plot of temporal evolution of plasma potential with $P_{13.56MHz}$. All the measurements have been carried at P_{2MHz}=2 00 W, $P_{12.56MHz}$ = 00 W and Ar pressure of 10 mTorr.

also increases due to the residual plasma density and it increases ion-neutral collision frequency, and therefore, decreases ambipolar diffusion constant. That, in turn, increases the τ_0. This is the reason that the stabilization time of plasma potential during pulse off phase increases with P_{2MHz} (see Figure 6).

The effect of $P_{13.56MHz}$ (P_{2MHz} = 200 W, $P_{12.56MHz}$ = 00 W) on the temporal evolution of plasma potential has been shown in figure 7 and shows similar trends as observed in figure 6. The time of occurrence of initial peaks decreases and the peak value increases with $P_{13.56MHz}$. A quick comparison between figures 6 and 7 reveals, for the total fixed RF power (P_{2MHz}+ $P_{13.56MHz}$), the plasma potential during 'initial peak' increases with the increasing P_{2MHz} content. All of these probe measurements have been carried out at the center of discharge, under the 2 MHz coil and ~ 200 mm radially away from 13.56 MHz coil. This is the reason that effects produced by P_{2MHz} is dominant at the probe location.

B. Effect of Substrate Biasing

Substrate biasing is an important technique used to control the energy of ions bombarding onto the substrate so that etching profile or thin film properties could be tailored. Therefore, an experimental study has been carried out to investigate the effect of substrate bias power on temporal evolution of plasma potential and the results are shown in figure 8. The 'P_{2MHz}' in pulsed mode and '$P_{13.56MHz}$' in CW mode have been kept constant at 200 W and the substrate bias power ($P_{12.56MHz}$) has been varied from 0 to 250 W. The floating potential of the probe is very sensitive to the balance of charged particles arriving at and leaving the probe. Probe responses to any fluctuation in the plasma varies at the time scale of inverse of ion plasma frequency. From the figure 8, it is clear that plasma potential rises to a very positive value of ~63 V when there is no bias power ($P_{12.56MHz}$ = 0 W) during the 'initial overshoot' and is highly unstable and therefore it quickly relaxes itself to a more homogeneous distribution. The reason of appearance of 'initial overshoot' depends upon the probe response and have been explained earlier. The magnitude of this 'initial overshoot' decreases with increasing bias power and reduces to ~ 55 V from ~ 63 V, when the bias power is increased from 0 W to 250 W. During 'stable on-phase', the plasma potential increases with increasing bias power. It increases from ~33 V to ~46 V, when bias power increases from 0 to 250 W. This increasing trend in the plasma potential due to the induced self-bias on the substrate.[34] The substrate is capacitively coupled to RF power. The RF voltage drop across the sheath developed adjacent to substrate elevates plasma potential during the whole pulse cycle ('ON' and 'OFF' phase). A fraction

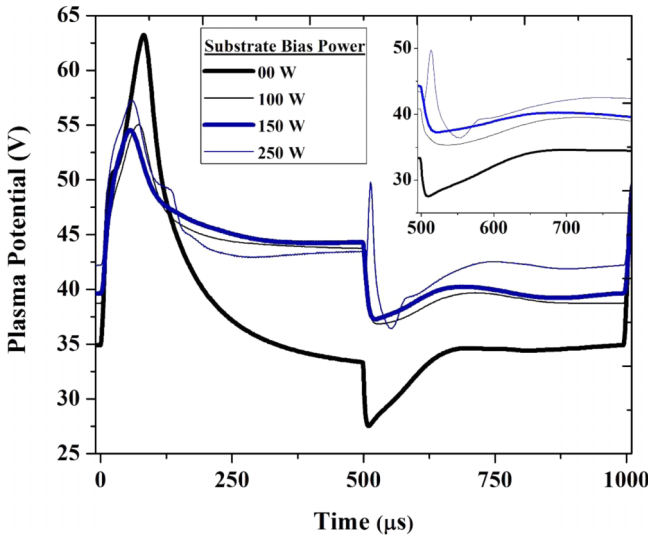

FIG. 8. A plot of temporal evolution of plasma potential with substrate bias power ($P_{12.56MHz}$). All the measurements have been carried at P_{2MHz} = 200 W, $P_{13.56MHz}$ = 200 W and Ar pressure of 10 mTorr.

of applied bias power deposited into the bulk plasma and it increases the bulk plasma density. The sheath formed around the substrate may also elevate the electron temperature. It has been observed in capacitive discharges that the electrons, those bounce back and forth between the two sheaths (electrostatic potential wells) can be heated by coherent interaction with RF fields.[35,36] Turner *et al.* demonstrated that electron heating produced either by collision-less or ohmic heating is much larger when the discharge is excited by a superposition of currents at frequencies than if either current acted as alone and it is due to due to coupling effects occurred because of low frequency current that strongly effects the discharge in sheath region.[37] Due to electron heating Bohm velocity $\left(\sqrt{\frac{kT_e}{M_i}}\right)$ at the sheath edge increases. The ion flux to the substrate is given by $J_i \sim qn_{is}\, v_{Bohm}$, where n_{is} is plasma density at the sheath edge. It means increased bias power increases ion flux to the substrate and it drains more ions from the plasma bulk towards the substrate and cause elevated plasma potential during 'on' and 'off' phase as observed. Alternatively, it can also be understood by relation between plasma potential (V_p), DC bias voltage (V_{DC}) and RF bias power. For a fixed electrode geometry, the VDC varies with RF current (Irf), which proportionally varies with RF bias power $V_{DC} \alpha I_{rf}$ and $I_{rf} \alpha P_{bias}$. The plasma potential $V_p \approx K.V_{DC}$, where K is constant which depends upon electrode geometry and scaling factor.[4] The I_{rf} increases with P_{bias}, which in turn, increases V_{DC} and it results in increased V_p as observed in the present study. The similar kind of plasma potential dependence upon bias power has also been observed in ECR plasmas.[38]

There is an interesting structure evolution in the plasma potential profile during the pulse 'off-time' as shown in figure 8. To investigate this feature more closely, a zoomed-in plot of pulse 'off-time' during t= 495 to 800 μs has been in the inset of figure 8. The plasma potential rapidly decreases from ~33 to ~27 V in ~10 μs as soon as P_{2MHz} switches off, then increases upto ~35 V in next ~150 μs and stabilizes for the rest of the cycle (for no biasing). The reason of this observation has been explained earlier on the basis of ambipolar diffusion processes occurring during pulse 'off-phase". The stabilization time of the plasma potential decreases with biasing power i.e. 150 μs for 0 W to 15 μs for 250 W and is due to the enhanced and faster diffusion of ions towards the substrate attributed as explained earlier. Due to quasi-neutrality of plasma, ambipolar diffusion is mainly determined by ion dynamics.[5] That is reason for decreasing stabilization time of plasma potential with increasing biasing power.

Beyond the 150 W of biasing power, an interesting feature in the evolution of the plasma potential, after the switching off P_{2MHz}, has been observed. Similar kind of structure in the plasma density and the plasma potential have been observed in other kinds of discharges.[39–41] Bradley *et al.*[39] suggested that it is due to the ion acoustic wave propagating towards substrate. A three

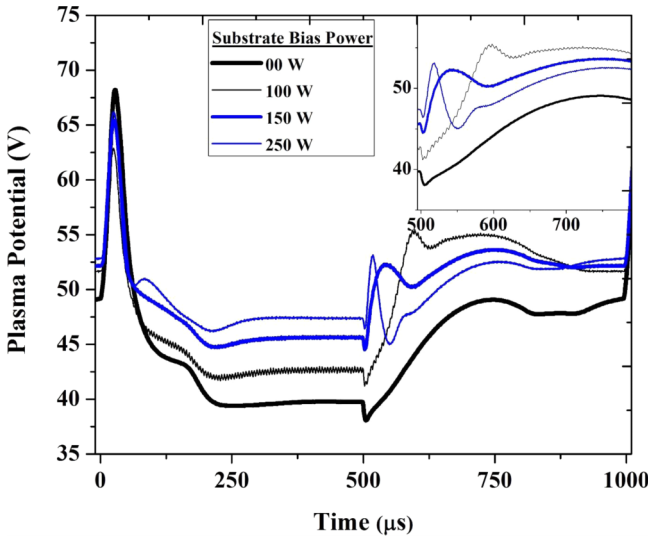

FIG. 9. A plot of temporal evolution of plasma potential with substrate bias power ($P_{12.56MHz}$). All the measurements have been carried at P_{2MHz} = 200 W, $P_{13.56MHz}$ = 600 W and Ar pressure of 10 mTorr.

step decay in plasma density during the pulse 'off-phase' has also been observed.[41] There is a need of further investigation to know the exact reason of this observation and why it occurs only after particular value of substrate bias power. However, it could be said, based on the studies[39–41] that this feature may be due to emergence of ion acoustic wave propagating towards the substrate.

Figure 9 shows the effect of substrate biasing power on plasma potential profile for P_{2MHz} = 200 W, $P_{13.56MHz}$ = 600 W conditions. A quick comparison of figures 8 and 9 reveals that the effect of $P_{13.56MHz}$ is to elevate the plasma potential in all of the substrate bias powers similar to the results in figure 7. Comparing the zoomed parts of 'off-phase' shown in the insets of figures 8 and 9, illustrates that stabilization time of the plasma potential also depends on $P_{13.56MHz}$ and increases with increasing $P_{13.56MHz}$.

IV. CONCLUSIONS

Using an emissive probe technique in a saturated floating potential mode, the measurement of temporal evolution of plasma potential has been carried out to investigate the effect of ICP power and bias power in dual frequency pulsed inductively coupled discharges produced by a dual-frequency dual-antenna ICP source.

Three distinct phases in plasma potential have been identified. Emergence of 'initial overshoot' could be attributed to the probe response time to plasma fluctuations. It has been found out that the plasma potential reduces with increasing P_{2MHz} during the whole cycle. However, plasma potential increases with $P_{13.56MHz}$. An interesting feature in plasma potential emerges with substrate biasing power and reason of this observation appears to be related to the ambipolar diffusion

ACKNOWLEDGEMENTS

This work was supported by the Industrial Strategic Technology Development Program (10041681, Development of fundamental technology for 10 nm process semiconductor and 10 G size large area process with high plasma density and VHF condition) funded by the Ministry of Knowledge Economy (MKE, Korea)

This work was also partly supported by the International Joint Research and Development Program (N009300229, Large area PECVD Equipment development for Flexible low temperature high density film deposition) funded by the Ministry of Knowledge Economy (MKE, Korea)

[1] C Y Chang and S M Sze, *ULSI Technology* (McGraw-Hill, New York, 1996), p. 329.
[2] J Hopwood, Plasma Sources Sci. Technol. **1**, 109 (1992).
[3] M Kahoh, K Suzuki, J Tonotani, K Aoki, and M Yamage, Jpn. J. Appl. Phys., Part 1 **40**, 5419 (2001).
[4] M. A. Lieberman and A. J. Lichtenberg, *Principles of Plasma Discharges and Materials Processing*, 2nd ed. (Wiley Interscience, New York, 2005).
[5] T Makabe and Z Petrovic, *Plasma Electronics: Applications in Microelectronic Device Fabrication* (Taylor and Francis, London, 2006).
[6] H H Goto, H D Lowe, and T Ohmi, J. Vac. Sci. Technol. A **10**(5), 3048 (1992).
[7] T Gans, J Schulze, D O'Connell, U Czarnetzki, R Faulkner, A R Ellingboe, and M M Turner, Appl. Phys. Lett. **89**, 261502 (2006).
[8] J Schulze, T Gans, D O'Connell, U Czarnetzki, A R Ellingboe, and M M Turner, J. Phys. D: Appl. Phys. **40**, 7008 (2007).
[9] J Schulze, Z Donko, D Luggenh olscher, and U Czarnetzki, Plasma Sources Sci. Technol. **18**, 034011 (2009).
[10] S K Ahn and H Y Chang, Appl. Phys. Lett. **95**, 111502 (2009).
[11] J P Booth, G Curley, D Maric, and P Chabert, Plasma Sources Sci. Technol. **19**, 015005 (2010).
[12] S H Lee, P K Tiwari, and J K Lee, Plasma Sources Sci.Technol. **18**, 025024 (2009).
[13] A C F Wu, M A Lieberman, and J P Verboncoeur, J. Appl.Phys. **101**, 056105 (2007).
[14] M A Lieberman, J P Booth, P Chabert, J M Rax, and M M Turner, Plasma Sources Sci. Technol. **11**, 283 (2007).
[15] G A Hebner, E V Barnat, P A Miller, A M Paterson, and J P Holland, Plasma Sources Sci. Technol. **15**, 879 (2006).
[16] P Chabert, J. Phys. D: Appl. Phys. **40**, R63 (2007).
[17] I Lee, D B Graves, and M A Lieberman, Plasma Sources Sci. Technol. **17**, 015018 (2008).
[18] A Mishra, K N Kim, T H Kim, and G Y Yeom, Plasma Source Sci. Technol. **21**, 035018 (2012).
[19] A Mishra, T H Kim, K N K. Kim, and G Y Yeom, J. Phys. D: Appl. Phys. **45**, 475201 (2012).
[20] A Mishra, T H Kim, K N Kim, and G Y Yeom, Plasma Sources Sci. Technol. **22**, 015022 (2013).
[21] J P Sheehan, Y Raitses, I Hershkowitz, and N J Fisch, Phys. Plasmas **18**, 073501 (2011).
[22] A Mishra, J S Seo, K N Kim, and G Y Yeom, J. Phys. D: Appl. Phys. **46**, 235203 (2013).
[23] G D Hobbs and J A Wesson, Plasma Phys. **9**, 85 (1967).
[24] E Y Wang, N Hershkowitz, T Intrator, and C Forest, Rev. Sci. Instr. **57**, 2425 (1986).
[25] A Mishra, P J Kelly, and J W Bradley, Plasma Sources Sci. Technol. **19**, 045014 (2010).
[26] A Mishra, P J Kelly, and J W Bradley, J. Phys. D: Appl. Phys. **44**, 425201 (2011).
[27] A Mishra, M H Jeon, K N Kim, and G Y Yeom, Plasma Sources Sci. Technol. **21**, 055006 (2012).
[28] J W Bradley, S K Karkari, and A Vetushka, Plasma Sources Sci. Technol. **13**, 189–198 (2004).
[29] V A Godyak, R B Piejak, and B M Alexandrovich, Plasma Sources Sci. Technol. **11**, 525 (2002).
[30] S Takamura, N Ohno, M Y Ye, and T Kubawara, Contrib. Plasma Phys. **1-3**, 126 (2004).
[31] A Marek, M Jilek, I Pickova, M Ticy, R Schrittwieser, and C Ionita, Contrib. Plasma Phys. **5-7**, 491 (2008).
[32] J W Bradley, S K Karkari, and A Vetushka, Plasma Sources Sci. Technol. **13**, 189 (2004).
[33] T Welzel, T Dunger, B Leibig, and F Richter, New J. Phys. **10**, 23008 (2008).
[34] R J Hoekstra and M J Kushner, J. Appl. Phys. D **79**(5), 2275 (1996).
[35] J Y Park and J K Lee, J. Appl. Phys. D **41**, 022004 (2008).
[36] Y-Xin Liu, Q-Zhi Zhang, J Liu, Y-Hong Song, A Boagaerts, and Y-Nian Wang, Plasma Sources Sci. Technol. **22**, 025012 (2013).
[37] M M Turner and P Chabert, Plasma Sources Science and Technol. **16**, 364 (2006).
[38] J H Pyo and K- X Woong, Journal of the Korean Physical Society **42**(February), S873–S875 (2003).
[39] J W Bradley and H Backer, Surface and Coating Technology **200**, 616 (2005).
[40] S H seo, J H In, and H Y Chang, Plasma Sources Sci. Technol. **15**, 256 (2006).
[41] J H In, B K Na, S H Seo, H Y Chang, and J G Han, Plasma Sources Sci. Technol. 045029 (2009).